PAPER

Uniqueness, stability and algorithm for an inverse wave-number-dependent source problem

IOP Publishing Inverse Problems
Inverse Problems **40** (2024) 125019 (25pp) https://doi.org/10.1088/1361-6420/ad8d75

Uniqueness, stability and algorithm for an inverse wave-number-dependent source problem

Mengjie Zhao[1], **Suliang Si**[2,*] **and Guanghui Hu**[3]

[1] School of Mathematics, Taiyuan University of Technology, 030024 Taiyuan, People's Republic of China
[2] School of Mathematics and Statistics, Shandong University of Technology, 255049 Zibo, People's Republic of China
[3] School of Mathematical Sciences and LPMC, Nankai University, 300071 Tianjing, People's Republic of China

E-mail: sisuliang@amss.ac.cn, zhaomengjie@tyut.edu.cn and ghhu@nankai.edu.cn

Received 18 April 2024; revised 30 September 2024
Accepted for publication 31 October 2024
Published 25 November 2024

Abstract

This paper is concerned with an inverse wave-number-/frequency-dependent source problem for the Helmholtz equation. In two and three dimensions, the unknown source term is supposed to be compactly supported in spatial variables but independent on one spatial variable. The dependence of the source function on wave-number/frequency is supposed to be unknown. Based on the Fourier-transform and Dirichlet-Laplacian methods, we develop two efficient non-iterative numerical algorithms to recover the wave-number-dependent source. Uniqueness proof and increasing stability analysis are carried out if the boundary measurement data of Dirichlet kind are available. Numerical experiments are conducted to illustrate the effectiveness and efficiency of the proposed methods.

Keywords: inverse source problem, wave-number-dependent source, Helmholtz equation, increasing stability

* Author to whom any correspondence should be addressed.

1. Introduction and motivations

1.1. Statement of the problem

Consider a time-dependent acoustic wave radiating problem in $\mathbb{R}^d$ ($d=2,3$) with the homogeneous initial conditions

$$\begin{cases} \partial_t^2 U(x,t) - \Delta U(x,t) = -S(x,t), & x \in \mathbb{R}^d, t>0, \\ U(x,0) = \partial_t U(x,0) = 0, & x \in \mathbb{R}^d, \end{cases} \tag{1.1}$$

where $x=(\tilde{x},x_d)$, $\tilde{x}=(x_1,x_2,\cdots,x_{d-1})\in\mathbb{R}^{d-1}$ and $U(x,t)$ represents the wave field. To state the motivation of our problem, we suppose that the source term $S(x,t)$ is excited by a moving point source along the trajectory $a(t):\mathbb{R}_+\longmapsto\mathbb{R}^d$ for $t\in[0,T]$, where $\mathbb{R}_+:=\{t\in\mathbb{R}:t\geqslant 0\}$. More precisely, we suppose that the source function takes the form (see e.g. [22])

$$S(x,t)=\delta\left(x-a\left(t\right)\right)\chi\left(t\right),x\in\mathbb{R}^d,t\in\mathbb{R}_+. \tag{1.2}$$

Here the symbol δ is the Dirac delta function and χ is the characteristic function over the interval $[0,T]$, given by

$$\chi\left(t\right)=\begin{cases} 1, & t\in[0,T], \\ 0, & t\notin[0,T]. \end{cases}$$

Assume further that the point source moves smoothly on the hyperplane $x_d=h$ for some $h>0$, so that the trajectory function can be rewritten as $a(t)=(\widetilde{a}(t),h)$, where $\widetilde{a}(t):\mathbb{R}_+\longmapsto\mathbb{R}^{d-1}$ is some smooth function. By (1.2), the source function can be rewritten as $S(x,t)=\delta(\tilde{x}-\widetilde{a}(t))\,\chi(t)\,\delta(x_d-h)$. Physically, the Delta function can be approximated by functions with a compact support in the distributional sense. Hence the source term $S(x,t)$ can be physically approximated by $F(\tilde{x},t)g(x_d)$, where F and g have compact supports. Below we shall identify $S(x,t)$ with $F(\tilde{x},t)g(x_d)$ for the convenience of mathematical analysis, that is, $S(x,t)=F(\tilde{x},t)g(x_d)$. The solution of problem (1.1) is given explicitly as

$$\begin{aligned} U(x,t) &= -\int_{\mathbb{R}^+}\int_{\mathbb{R}^d} G_d\left(x-y;t-\tau\right)S\left(y,\tau\right)\mathrm{d}y\mathrm{d}\tau \\ &= -\int_{\mathbb{R}^+}\int_{\mathbb{R}^d} G_d\left(x-y;t-\tau\right)F\left(\tilde{y},t\right)g\left(x_d\right)\mathrm{d}y\mathrm{d}\tau \end{aligned}$$

for all $x\in\mathbb{R}^d$ and $t>0$, where

$$G_d\left(x;t\right)=\begin{cases} \dfrac{H(t-|x|)}{2\pi\sqrt{t^2-|x|^2}}, & d=2,\quad |x|\neq t, \\ \dfrac{\delta\left(t-|x|\right)}{4\pi|x|}, & d=3,\quad |x|\neq t,\ |x|\neq 0, \end{cases} \qquad x\in\mathbb{R}^d, t>0$$

is the fundamental solution to the wave equation in $\mathbb{R}^d$ and H is the Heaviside function

$$H\left(\tau\right)=\begin{cases} 1, & \text{if}\quad \tau\geqslant 0, \\ 0, & \text{if}\quad \tau<0. \end{cases}$$

The n-dimensional ($n = 1, 2$) Fourier and inverse Fourier transforms in this paper are defined respectively by

$$(\mathcal{F}_\xi \rho)(\tau) = \frac{1}{(2\pi)^{n/2}} \int_{\mathbb{R}^n} \rho(\xi) \mathrm{e}^{-\mathrm{i}\tau\cdot\xi} \mathrm{d}\xi, \quad \tau \in \mathbb{R}^n,$$
$$\left(\mathcal{F}_\tau^{-1} q\right)(\xi) = \frac{1}{(2\pi)^{n/2}} \int_{\mathbb{R}^n} q(\tau) \mathrm{e}^{\mathrm{i}\tau\cdot\xi} \mathrm{d}\tau, \quad \xi \in \mathbb{R}^n,$$

where the subscript denotes the variable to be Fourier or inverse Fourier transformed. The inverse Fourier transform of the source term can be expressed as

$$\left(\mathcal{F}_t^{-1} F\right)(\tilde{x}, k)\, g(x_d) := f(\tilde{x}, k)\, g(x_d).$$

It is obvious that the spatial function $\tilde{x} \longmapsto f(\tilde{x}, k)$ is compactly supported for all $k > 0$. The temporal inverse Fourier transform of $U(x, \cdot)$ is given by

$$u(x, k) := \left(\mathcal{F}_t^{-1} U\right)(x, k) = -\frac{1}{\sqrt{2\pi}} \int_{\mathbb{R}^d} \Phi_d(x - y; k) f(\tilde{y}, k)\, g(y_d) \mathrm{d}y, \qquad x \in \mathbb{R}^d, k > 0, \quad (1.3)$$

where $\Phi_d(x; k)$ is the fundamental solution to the Helmholtz equation $(\Delta + k^2)u = 0$ in $\mathbb{R}^d$, given by

$$\Phi_d(x - y; k) = \left(\mathcal{F}_t^{-1} G_d\right)(x - y; k) = \begin{cases} \dfrac{\mathrm{i}}{4} H_0^{(1)}(k|x - y|), & d = 2, \\ \dfrac{\mathrm{e}^{\mathrm{i}k|x-y|}}{4\pi|x - y|}, & d = 3, \end{cases} \qquad x, y \in \mathbb{R}^d,\ x \neq y.$$

Here $H_0^{(1)}$ is the first kind Hankel function of order zero. Applying the inverse Fourier transform with respect to the time variable to the wave equation (1.1), one obtains

$$\Delta u(x, k) + k^2 u(x, k) = f(\tilde{x}, k)\, g(x_d), \qquad x = (\tilde{x}, x_d) \in \mathbb{R}^d, k > 0. \quad (1.4)$$

Moreover, the radiated field $u(\cdot, k)$ satisfies the Sommerfeld radiation condition at infinity

$$\lim_{r\to\infty} r^{\frac{d-1}{2}} (\partial_r u - \mathrm{i}ku) = 0, r = |x|, \quad (1.5)$$

which holds uniformly in all directions $\hat{x} = x/|x| \in \mathbb{S}^{d-1} := \{x \in \mathbb{R}^d : |x| = 1\}$.

Denote by $B_R \subset \mathbb{R}^d$ the sphere centered at the origin with the radius $R > 0$ and by $\partial B_R := \{x \in \mathbb{R}^d : |x| = R\}$ the boundary of B_R. The unit normal vector ν at the boundary ∂B_R is supposed to direct into the exterior of B_R.

We make the following assumptions on the source functions $f(\tilde{x}, k)$ and $g(x_d)$:

Assumption 1.1. (a) There exist a subdomain $\widetilde{D} \subset \mathbb{R}^{d-1}$ and a subinterval $H \subset \mathbb{R}_+$ such that $\operatorname{supp} g = \overline{H}$, $\operatorname{supp} f(\cdot, k) = \overline{\widetilde{D}}$, $(\widetilde{D} \times H) \subset\subset B_R$.
(b) $f(\cdot, k) \in L^2(\widetilde{B}_R)$, where $\widetilde{B}_R := \{\tilde{x} \in \mathbb{R}^{d-1} : |\tilde{x}| < R\}$ and $g \in L^2(-R, R)$.
(c) The source function $f(\tilde{x}, k)$ is analytic with respect to k, g is *a priori* known and $g \not\equiv 0$.

In this paper, we are interested in the following inverse problem:
(IP): Determine the source function $\tilde{x} \mapsto f(\tilde{x}, k) \in L^2(\widetilde{B}_R)$ for all $k > 0$ from knowledge of the multi-frequency near-field measurement

$$\{u(x, k) : x \in \partial B_R,\ k \in [k_{\min}, k_{\max}]\}, \quad (1.6)$$

where $[k_{\min}, k_{\max}]$ denotes an interval of available wave-numbers with $0 < k_{\min} < k_{\max}$.

1.2. Literature review

Inverse source problems in wave propagation are of great importance in various scientific and engineering fields such as antenna design and synthesis, medical imaging and photo-acoustic tomography [3, 18, 21, 31]. Consequently, a great deal of mathematical and numerical results are available, especially for wave-number-independent source problems of the Helmholtz equation. In general, there is an obstruction to uniqueness for inverse source problems with single-frequency data due to the existence of non-radiating sources [10, 26]. Computationally, a more serious issue is the stability analysis, i.e. to quantify how does a small variation of the data lead to a huge error in the reconstruction. Hence it is crucial to study the stability of inverse source problems. Recently, it has been realized that the use of multi-frequency data is an effective approach to overcome the difficulties of non-uniqueness and instability which are encountered at a single frequency. In [5], Bao *et al* initialized the mathematical study on the stability of inverse wave-number-independent source problems for the Helmholtz equation by using multi-frequency data. In the recent works [4, 5, 11, 15, 23], uniqueness and stability results have been proved for recovering source terms from multi-frequency boundary measurements. In [5], the authors treated an interior inverse source problem for the Helmholtz equation from boundary Cauchy data at multiple wave-numbers and showed an increasing stability estimate. A uniqueness result and numerical algorithm for recovering the location and shape of a supported acoustic source function from boundary measurements at many frequencies were shown in [11]. The approach of [15] also provides inspirations for establishing uniqueness result. It was shown that an acoustic source of the form $S(x,k) = f(x)g(k)$ can be identified uniquely by boundary measurements of the acoustic field. The proof relies on complete sets of solutions to the homogeneous Helmholtz equation. An error estimate and a numerical algorithm for the solution are presented. Several numerical methods for solving the multi-frequency inverse source problem have been proposed. We refer the reader to [6, 32] for the Fourier method and recursive algorithm. In addition, there are other uniqueness, increasing stability and algorithm results; see also [1, 2, 7, 8, 9, 12, 16, 17, 24, 25, 27–29] and the references therein.

To the best of our knowledge, there are only few works on inverse wave-number-dependent source problems. Even using multi-frequency data, there is no uniqueness in recovering general wave-number-dependent (or frequency-dependent) source functions. Difficulties arise from the fact that the far-field measurement data are no longer the Fourier transform form of the source function. The wave-number-dependent source functions are closely connected to time-dependent source functions in the time domain [19, 22, 23]. We refer to [19, 20] for sampling methods to image the support of a special class of wave-number-dependent source functions with known radiating periods. In this paper, we consider acoustic source functions of the form $f(\tilde{x},k)g(x_d)$ in the frequency regime. The unknown wave-number-dependent source function f is independent of one spatial variable and the source term $g(x_d)$, $x_d \in \mathbb{R}$ is supposed to be *a priori* known. Motivated by existing results for wave-number-independent sources [5, 11, 15, 25, 28], we prove uniqueness and increasing stability in covering the source function $\tilde{x} \mapsto f(\tilde{x},k)$, $\tilde{x} \in \mathbb{R}^{d-1}$ from the Dirichlet boundary data (1.6) at a fixed wave-number/frequency $k > 0$. This implies that the multi-wave-number/frequency data can be used to uniquely identify the function f by the analytic continuation w.r.t. k. Inspired by the idea of [15], we choose a complete orthonormal set to prove that the source function f can be identified uniquely by the Dirichlet data measured on the boundary; see the uniqueness result shown in theorem 2.2. The uniqueness proof and inversion algorithms are based on two methods: Fourier-transform method and Dirichlet-Laplacian method. The increasing stability estimates are derived from the Fourier-transform method and the technique of [11].

The remaining part of the paper is organized as follows. In section 2, we show that the source term $f(\tilde{x},k)$ can be identified uniquely by the multi-frequency near-field data. Section 3 is devoted to the increasing stability analysis. Numerical experiments are presented in section 4 to verify the effectiveness of the proposed two methods.

2. Uniqueness

This section is concerned with uniqueness of the inverse wave-number-dependent source problem by measuring the near-field acoustic field at many frequencies. In subsection 2.1 we prove uniqueness by applying the Fourier-transform method with test functions, while subsection 2.2 shows an alternative proof based on the Dirichlet-Laplacian method.

2.1. Uniqueness via Fourier-transform method

In this subsection, we aim to prove uniqueness by applying the Fourier-transform method. The uniqueness result is stated as follows.

Theorem 2.1. *Suppose that the source functions f and g satisfy the assumption 1.1 and that $u(\cdot,k)\in H^2(B_R)$ for all $k>0$ is the unique solution to the inhomogeneous Helmholtz equation (1.4) with the Sommerfeld radiation condition (1.5). Then the source term $\tilde{x}\mapsto f(\tilde{x},k)\in L^2(\widetilde{B}_R)$ for all $k>0$ can be uniquely determined by the Dirichlet data $\{u(x,k):x\in \partial B_R,\ k\in[k_{\min},k_{\max}]\}$.*

Proof. Since the inverse source problem is linear and g is *a priori* known, we shall prove $f\equiv 0$ by assuming $u(x,k)=0$ on ∂B_R for all $k\in[k_{\min},k_{\max}]$. Recalling uniqueness of the exterior boundary value problem of the Helmholtz equation [30, theorems 9.10 and 9.11], one can conclude that $u(\cdot,k)=0$ in $\mathbb{R}^d\overline{B}_R$ and thus $\partial_\nu u(x,k)=0$ on ∂B_R for $k\in[k_{\min},k_{\max}]$. Define the wave-number-dependent test functions

$$\psi(x,k)=\mathrm{e}^{-\mathrm{i}\xi\cdot x},\xi=\left(\tilde{\xi},\xi_d\right)\in\mathbb{R}^d,|\xi|=k. \tag{2.7}$$

It is easy to verify $\Delta\psi(x,k)+k^2\psi(x,k)=0$ in $\mathbb{R}^d$. Multiplying $\psi(\cdot,k)$ on both sides of (1.4) and integrating over B_R, we obtain

$$\begin{aligned}\int_{B_R} f(\tilde{x},k)\,g(x_d)\,\psi(x,k)\,\mathrm{d}x&=\int_{B_R}\left(\Delta u(x,k)+k^2u(x,k)\right)\psi(x,k)\,\mathrm{d}x,\\&=\int_{\partial B_R}\left[\frac{\partial u(x,k)}{\partial\nu(x)}\psi(x,k)-u(x,k)\frac{\partial\psi(x,k)}{\partial\nu(x)}\right]\mathrm{d}s(x)\\&=0.\end{aligned} \tag{2.8}$$

By our *a priori* information on f, we obtain

$$\left(\int_{\widetilde{D}} f(\tilde{x},k)\,\mathrm{e}^{-\mathrm{i}\tilde{\xi}\cdot\tilde{x}}\mathrm{d}\tilde{x}\right)\left(\int_H g(x_d)\,\mathrm{e}^{-\mathrm{i}\xi_d x_d}\mathrm{d}x_d\right)=0,\quad k\in[k_{\min},k_{\max}].$$

Below we fix some $k\in[k_{\min},k_{\max}]$. Noting that $\operatorname{supp} g(x_d)=\overline{H}$ and $g\not\equiv 0$ by assumption 1.1, one can always find some $0<\eta<k$ such that $(\mathcal{F}g)(\xi_d)\neq 0$ for all $\xi_d\in(0,\eta)$. Define $S_k:=\{\tilde{\xi}\in\mathbb{R}^{d-1}:\ |\tilde{\xi}|^2=k^2-\xi_d^2\}$ for some fixed $\xi_d\in(0,\eta)$. Then it follows from the previous relation that

$$\int_{\widetilde{D}} f(\tilde{x},k)\,\mathrm{e}^{-\mathrm{i}\tilde{\xi}\cdot\tilde{x}}\mathrm{d}\tilde{x}=0\quad\text{for all}\quad\tilde{\xi}\in S_k. \tag{2.9}$$

From (2.9), we deduce that $(\mathcal{F}_{\tilde{x}}f)(\tilde{\xi},k)=0$ for all $\tilde{\xi}\in S_k$ with every fixed $k\in[k_{\min},k_{\max}]$. Consequently, one obtains $(\mathcal{F}_{\tilde{x}}f)(\tilde{\xi},k)=0$ for all $\tilde{\xi}\in\mathbb{R}^{d-1}$, since $\mathcal{F}_{\tilde{x}}f$ is analytic in $\mathbb{R}^{d-1}$ and S_k is a non-empty open subset of $\mathbb{R}^{d-1}$. Taking the inverse Fourier transform on $(\mathcal{F}_{\tilde{x}}f)(\tilde{\xi},k)$ yields $\mathcal{F}_{\tilde{\xi}}^{-1}(\mathcal{F}_{\tilde{x}}f)=f(\tilde{x},k)=0$ for all $\tilde{x}\in\mathbb{R}^{d-1}$ with an arbitrarily fixed $k\in[k_{\min},k_{\max}]$. Finally, we conclude that $f(\tilde{x},k)=0$ with $\tilde{x}\in\mathbb{R}^{d-1}$ for all $k>0$ by applying the analyticity of $f(\tilde{x},k)$ with respect to k. □

2.2. Uniqueness via Dirichlet-Laplacian method

The proof presented in section 2.1 cannot be directly applied to inhomogeneous background media, due to the difficulties in constructing test functions. Here we explore an alternative method based on the completeness of Dirichlet eigenfunctions for the negative Laplacian. Let $v\in H_0^1(\widetilde{B}_R)$ be an eigenfunction of the Dirichlet Laplacian in $\widetilde{B}_R$, i.e. a non-trivial solution to the Dirichlet problem of the homogeneous Helmholtz equation in $\widetilde{B}_R$,

$$-\Delta_{\tilde{x}}v(\tilde{x})=\lambda^2 v(\tilde{x}),\quad \tilde{x}\in\widetilde{B}_R,\qquad v(\tilde{x})=0,\ \tilde{x}\in\partial\widetilde{B}_R.$$

Here λ^2 is known as the Dirichlet eigenvalue over the subdomain $\widetilde{B}_R$ in $\mathbb{R}^{d-1}$. Denote the sequence of eigenvalues as $\{\lambda_m^2\}_{m\in\mathbb{N}^+}$ counted with their multiplicity and the Dirichlet eigenfunctions as $\{v_j^{(m)}\}_{j=1}^{l_m}$ with $l_m\in\mathbb{N}^+$ associated with λ_m^2. We renumber all eigenfunctions as $\{v_n\}_{|n|\in\mathbb{N}^+}$ for simplicity. Since the Dirichlet Laplacian operator is positive and self-adjoint over the space $L^2(\widetilde{B}_R)$, the set of eigenfunctions $\{v_n\}_{|n|\in\mathbb{N}^+}$ forms a complete orthonormal basis in $L^2(\widetilde{B}_R)$. Thus for all $h\in L^2(\widetilde{B}_R)$ we have the convergent expansion

$$h(y)=\sum_{|n|\in\mathbb{N}^+}h_n\,v_n(y),\quad y\in\widetilde{B}_R,\tag{2.10}$$

where the coefficients h_n are given by

$$h_n=\int_{\widetilde{B}_R}h(y)\,\bar{v}_n(y)\,\mathrm{d}y,\quad |n|\in\mathbb{N}^+.$$

We remark that the only possible accumulating point of λ_n^2 is at infinity.

Lemma 2.1. *Let $\{\lambda_n^2\}_{n=1}^{+\infty}$ be the sequence of Dirichlet eigenvalues over $\widetilde{B}_R$. Then there exists an open subinterval $K\subset[k_{\min},k_{\max}]$ such that $\lambda_n\notin K$ and the relation*

$$\int_H g(t)\,e^{\sqrt{\lambda_n^2-k^2}\,t}\,dt\neq 0\quad \textit{for all}\quad k\in K$$

holds for all $n\in\mathbb{N}^+$.

Proof. Suppose on the contrary that for any subinterval $K\subset[k_{\min},k_{\max}]$ which satisfies $\lambda_n\notin K$ for all $n\in\mathbb{N}^+$, one can always find an eigenvalue λ_l, $l\in\mathbb{N}^+$ such that

$$\int_H g(t)\,\mathrm{e}^{\sqrt{\lambda_l^2-k^2}\,t}\,\mathrm{d}t=0,\quad \forall\,k\in K.\tag{2.11}$$

For the aforementioned $l\in\mathbb{N}^+$, we introduce two subsets of K:

$$K_1:=\{k\in K:\ k^2<\lambda_l^2\},\quad K_2:=\{k\in K:\ k^2>\lambda_l^2\}.$$

It is obvious that K_1 and K_2 cannot be both empty. We consider the following two cases.

Case (i): $K_1 \subset K$ is non-empty. Introducing the variable $s := \sqrt{\lambda_l^2 - k^2}$ for $k \in K_1$, one obtains $s \in (c,d)$ for some $0 \leqslant c < d < \infty$. Observing that the function $s \longmapsto \int_H g(t)\mathrm{e}^{st}\,\mathrm{d}t$ is analytic with respect to $s \in \mathbb{R}$ and applying the Taylor expansion for the exponential function, we obtain

$$0 = \int_H g(t)\,\mathrm{e}^{st}\mathrm{d}t = \sum_{n\in\mathbb{N}} A_n s^n, \qquad A_n := \frac{1}{n!}\int_H g(t)\,t^n\,\mathrm{d}t, \quad n \in \mathbb{N}$$

for all $s \in \mathbb{R}$, and hence $A_n = 0$. This together with the completeness of polynomials in $L^2(H)$ implies $g = 0$, which is a contradiction to our assumption $g \not\equiv 0$.

Case (ii): $K_2 \subset K$ is non-empty. In this case one obtains

$$\int_H g(t)\,\mathrm{e}^{\sqrt{\lambda_l^2-k^2}\,t}\mathrm{d}t = \int_H g(t)\,\mathrm{e}^{\mathrm{i}\sqrt{k^2-\lambda_l^2}\,t}\mathrm{d}t = \left(\mathcal{F}_t^{-1}g\right)\left(\sqrt{k^2-\lambda_l^2}\right) = 0, \quad k \in K_2.$$

Again using the analyticity of the inverse Fourier transform of g, we conclude that $(\mathcal{F}_t^{-1}g) = 0$ in $\mathbb{R}$. Therefore, we get $\mathcal{F}_k(\mathcal{F}_t^{-1}g) = g = 0$ in $\mathbb{R}$, which contradicts the assumption $g \not\equiv 0$.

□

Below we present the second uniqueness proof, which differs from the proof of theorem 2.1 in the choice of test functions.

Theorem 2.2. *Under the assumption of theorem 2.1, the source function $\tilde{x} \mapsto f(\tilde{x},k) \in L^2(\widetilde{B}_R)$ for all $k > 0$ can be uniquely determined by the Dirichlet data $\{u(x,k) : x \in \partial B_R,\ k \in [k_{\min}, k_{\max}]\}$.*

Proof. Define the k-dependent test functions

$$\varphi_n(x,k) = v_n(\tilde{x})\ \mathrm{e}^{\sqrt{\lambda_n^2-k^2}\,x_d}, \quad n \in \mathbb{N}^+,$$

where λ_n^2 are the Dirichlet eigenvalues and v_n is chosen as any Dirichlet eigenfunction associated with λ_n^2. For all $n \in \mathbb{N}^+$, the function φ_n satisfies the Helmholtz equation $\Delta\varphi_n(x,k) + k^2\varphi_n(x,k) = 0$ in $\widetilde{B}_R$.

Assuming $u(x,k) = 0$ on $\partial\mathrm{B}_R$ for $k \in [k_{\min}, k_{\max}]$, we deduce that $\partial_\nu u(x,k) = 0$ on $\partial\mathrm{B}_R$ for $k \in [k_{\min}, k_{\max}]$. Multiplying $\varphi_n(\cdot,k)$ on both sides of (1.4) and integrating over B_R for all $n \in \mathbb{N}^+$, we obtain

$$\begin{aligned}\int_{B_R} f(\tilde{x},k)\,g(x_d)\,\varphi_n(x,k)\,\mathrm{d}x &= \int_{B_R}\left(\Delta u(x,k) + k^2 u(x,k)\right)\varphi_n(x,k)\,\mathrm{d}x \\ &= \int_{\partial B_R}\left(\frac{\partial u(x,k)}{\partial\nu(x)}\varphi_n(x,k) - u(x,k)\,\frac{\partial\varphi_n(x,k)}{\partial\nu(x)}\right)\mathrm{d}s(x) \\ &= 0,\end{aligned} \tag{2.12}$$

which leads to the relation

$$\left(\int_{\widetilde{D}} f(\tilde{x},k)\,v_n(\tilde{x})\,\mathrm{d}\tilde{x}\right)\cdot\left(\int_H g(x_d)\,\mathrm{e}^{\sqrt{\lambda_n^2-k^2}\,x_d}\mathrm{d}x_d\right) = 0$$

for all $n \in \mathbb{N}^+$, $k \in [k_{\min}, k_{\max}]$. By lemma 2.1, there exists an open subinterval $K \subset [k_{\min}, k_{\max}]$ such that

$$\int_H g(x_d)\,\mathrm{e}^{\sqrt{\lambda_n^2-k^2}\,x_d}\mathrm{d}x_d \neq 0, \quad \forall\, k \in K$$

holds for all $n \in \mathbb{N}^+$. This implies the relation

$$\int_{\widetilde{B}_R} f(\tilde{x},k)\, v_n(\tilde{x})\, \mathrm{d}\tilde{x} = 0, \quad k \in K \tag{2.13}$$

for all $n \in \mathbb{N}^+$. Recalling the completeness of the orthonormal basis $\{v_n\}_{|n|\in\mathbb{N}^+}$ in $L^2(\widetilde{B}_R)$, we get $f(\tilde{x},k) = 0$ for all $\tilde{x} \in \widetilde{B}_R$ and $k \in K$. The analyticity of f in k yields the vanishing of $f(\cdot,k)$ for all $k \in \mathbb{R}$.

□

3. Increasing stability in two dimensions

In this section we restrict our discussions to the two dimensional settings (i.e. $d = 2$) and perform a stability analysis for recovering the wave-number-dependent source $f(x_1,k)$ with explicit dependence on the wave-number $k \geqslant 1$, which is also well known as the increasing stability with respect to k. We retain the notations used in the previous sections. For notational convenience, we write $f_k(x_1) := f(x_1,k)$, which is supported in the interval $(-R,R)$.

Introduce the Dirichlet-to-Neumann (DtN) operator $\mathcal{B} : H^{1/2}(\partial B_R) \to H^{-1/2}(\partial B_R)$ by $\mathcal{B}(u|_{\partial B_R}) = \frac{\partial u}{\partial \nu}|_{\partial B_R}$, where u is the solution to our source problem. Using the DtN operator, we can reformulate the Sommerfeld radiation condition into a transparent boundary condition $\frac{\partial u}{\partial \nu} = \mathcal{B}u$ on ∂B_R, where ν is the unit outer normal on ∂B_R. Below we shall derive an upper bound of $\mathcal{B}$ with explicit dependance on the wave-number k, based on the result of [14]. It is worth mentioning that the estimate for the upper bound also applies to DtN operators defined on a non-circular closed boundary, although the transparent operator $\mathcal{B}$ is defined on a circle within this paper.

Let $\widetilde{R} > R$. We denote $D = \{x \in \mathbb{R}^2 \setminus \overline{B_R} : |x| < \widetilde{R}\}$ and $V := \{v \in H^1(D) : v = 0 \text{ on } |x| = R\}$ equipped with the norm

$$\|v\|_V := \left(\int_D \left(|\nabla v|^2 + k^2 |v|^2 \right) \mathrm{d}x \right)^{1/2}.$$

Consider the exterior boundary value problem:

$$\begin{cases} \Delta u(x) + k^2 u(x) = 0, \ x \in \mathbb{R}^2 \setminus \overline{B_R}, \\ u = h, \ x \in \partial B_R, \\ \lim\limits_{r\to\infty} r^{\frac{1}{2}} (\partial_r u - iku) = 0, \quad r = |x|, \end{cases} \tag{3.14}$$

where $h \in H^{1/2}(\partial B_R)$. Using the integral equation or variational approach, one can prove that the problem (3.14) has a unique solution $u \in H^1_{\mathrm{loc}}(\mathbb{R}^2 \setminus \overline{B_R})$, even if the boundary ∂B_R is not circular; see e.g. [13, chapter 3]. By the extension theory in Sobolev spaces, there exists some $w \in H^1_{\mathrm{loc}}(\mathbb{R}^2 \setminus \overline{B_R})$ satisfying $w|_{\partial B_R} = h$ and $\|w\|_{H^1(D)} \leqslant C\|h\|_{H^{1/2}(\partial B_R)}$. Choose a cut-off function $\chi \in C^\infty(\mathbb{R}^2)$ satisfying $\chi = 0$ in $|x| > \frac{R+\widetilde{R}}{2}$ and $\chi = 1$ in $|x| \leqslant R$.

It is easy to see that the function $\widetilde{u} := u - \chi w$ satisfies

$$\begin{cases} \Delta \widetilde{u} + k^2 \widetilde{u} = -\left(\Delta + k^2\right)(\chi w), \ x \in \mathbb{R}^2 \setminus \overline{B_R}, \\ \widetilde{u} = 0, \ x \in \partial B_R. \end{cases}$$

The right hand side $(\Delta + k^2)(\chi w)$ belongs to the space $H^{-1}(D)$, the dual space of $H_0^1(D)$. According to lemma 3.3 in [14], we get the following estimate of $\widetilde{u}$:

$$\|\widetilde{u}\|_V \leqslant \left(5 + 4\sqrt{2}k\widetilde{R}\right) \| \left(\Delta + k^2\right)(\chi w) \|_{V^*}. \tag{3.15}$$

Applying the Cauchy–Schwartz inequality and the definition of V^*, we deduce that

$$\begin{aligned} \| \left(\Delta + k^2\right)(\chi w) \|_{V^*} &= \sup_{\|\varphi\|_V \leqslant 1} \langle \left(\Delta + k^2\right)(\chi w), \varphi \rangle_{L^2(D)} \\ &= \sup_{\|\varphi\|_V \leqslant 1} \int_D \left(-\nabla(\chi w) \cdot \nabla \overline{\varphi} + k^2 \chi w \cdot \overline{\varphi}\right) \mathrm{d}x \\ &\leqslant Ck^2 \|w\|_{H^1(D)}, \end{aligned}$$

where $C > 0$ depends on $\widetilde{R}$,R and we have used the fact $k^2 \geqslant 1$. Combining the above inequality and (3.15), it follows that

$$\|\widetilde{u}\|_V \leqslant C\left(5 + 4\sqrt{2}k\widetilde{R}\right) k^2 \|w\|_{H^1(D)} \leqslant C_1 k^3 \|w\|_{H^1(D)}$$

for some constant C_1 independent of k. Noting that $k \geqslant 1$, we have

$$\|\widetilde{u}\|_{H^1(D)} \leqslant \|\widetilde{u}\|_V \leqslant C_1 k^3 \|w\|_{H^1(D)}.$$

Therefore we obtain

$$\begin{aligned} \|u\|_{H^1(D)} = \|\widetilde{u} + \chi w\|_{H^1(D)} &\leqslant \|\widetilde{u}\|_{H^1(D)} + \|\chi w\|_{H^1(D)} \\ &\leqslant Ck^3 \|h\|_{H^{1/2}(\partial B_R)}, \end{aligned} \tag{3.16}$$

where $C > 0$ is independent of k. By the trace theorem, it holds that

$$\left\| \frac{\partial u}{\partial \nu} \right\|_{H^{-1/2}(\partial B_R)} \leqslant C\|u\|_{H^1(D)}$$

for some positive constant C depending on $\widetilde{R}$ and R. Therefore,

$$\|\mathcal{B}u\|_{H^{-1/2}(\partial B_R)} = \left\| \frac{\partial u}{\partial \nu} \right\|_{H^{-1/2}(\partial B_R)} \leqslant Ck^3 \|u\|_{H^{1/2}(\partial B_R)}, \tag{3.17}$$

where $C > 0$ is independent of k. Thus (3.17) gives an explcit upper bound estimate of $\mathcal{B}$ with respect to k. Numerically, one can also explicitly obtain the Neumann data on ∂B_R once the Dirichlet data is available on ∂B_R, because the operator $\mathcal{B}$ can be rewritten in a series form; see section 4 for the details.

For the stability estimate we make an additional assumption that there exists a constant δ such that

$$|\widehat{g}(\xi_2)| \geqslant \delta > 0 \quad \text{for all} \quad \xi_2 \in (-k, k), \tag{3.18}$$

where $\widehat{g}$ denotes the one-dimensional Fourier transform of g. Physically, the condition (3.18) means that the frequencies of the x_2-dependent source function g are mostly restricted to the interval $(-k, k)$. The main increasing stability result is shown below, which is also valid in three dimensions.

Theorem 3.1. *Let $u(\cdot,k)$ be the unique solution to the problem (1.4) and (1.5) with $\|f_k\|_{H^1(\mathbb{R})} \leqslant M$ for some $M > 1$. Assume that (3.18) holds. Then there exists a constant $C(R,\delta) > 0$ such that*

$$\|f_k\|^2_{L^2(\mathbb{R})} \leqslant C\left(k^9\epsilon^2 + \frac{M^2}{k^{\frac{4}{3}}|\ln\epsilon|^{\frac{1}{2}}}\right), \tag{3.19}$$

where $k \geqslant 1$ and $\epsilon = \|u\|_{H^{1/2}(\partial B_R)}$.

Remark 3.1. In theorem 3.1 the wave-number $k \geqslant 1$ is fixed. Obviously, one can get the uniqueness in recovering f_k as a consequence of the above stability estimate. The right hand side of (3.19) consists of two parts: the Lipschitz type data discrepancy and the high frequency tail of the source functions. As the frequency k increases, the latter decreases and thus becomes negligible. The result reveals that the inverse problem becomes more stable when higher frequency data are used. Additionally, we remark that only the Dirichlet boundary data are involved on the right hand of (3.19).

The proof of theorem 3.1 is motivated by the uniqueness proof of theorem 2.1 and the increasing stability for wave-number-independent source functions [11, 28].

Let $\xi = (\xi_1,\xi_2) \in \mathbb{R}^2$ with $|\xi| = k$. Multiplying $\mathrm{e}^{-\mathrm{i}(\xi_1 x_1 + \xi_2 x_2)}$ on both sides of (1.4) and integrating over $B_R \subset (-R,R)^2$, we obtain (see (2.8))

$$\left(\int_{-R}^{R} f(x_1,k)\,\mathrm{e}^{-\mathrm{i}\xi_1 x_1}\mathrm{d}x_1\right)\left(\int_{-R}^{R} g(x_2)\,\mathrm{e}^{-\mathrm{i}\xi_2 x_2}\mathrm{d}x_2\right) = \int_{\partial B_R} \mathrm{e}^{-\mathrm{i}\xi\cdot x}\left(\partial_\nu u + i\xi\cdot\nu u\right)\mathrm{d}s(x), \tag{3.20}$$

Using the estimate of the Neumann data (3.17), we bound the first term on the right hand of (3.20) by

$$\begin{aligned}\int_{\partial B_R} \mathrm{e}^{-\mathrm{i}\xi\cdot x}\left(\partial_\nu u\right)\mathrm{d}s(x) &\leqslant \|\partial_\nu u\|_{H^{-1/2}(\partial B_R)}\|\mathrm{e}^{-\mathrm{i}\xi\cdot x}\|_{H^{1/2}(\partial B_R)}\\ &\leqslant \|\partial_\nu u\|_{H^{-1/2}(\partial B_R)}\|\mathrm{e}^{-\mathrm{i}\xi\cdot x}\|_{H^{1}(\partial B_R)}\\ &\leqslant Ck^4\|u\|_{H^{1/2}(\partial B_R)}.\end{aligned}$$

The second term can be estimated analogously. Combining the above inequality and (3.18), (3.20), we conclude that

$$\begin{aligned}\left|\int_{-R}^{R} f(x_1,k)\,\mathrm{e}^{-\mathrm{i}\xi_1 x_1}\mathrm{d}x_1\right|^2 &\leqslant C\left|\int_{\partial B_R} \mathrm{e}^{-\mathrm{i}\xi\cdot x}\left(\partial_\nu u + i\xi\cdot\nu u\right)\mathrm{d}s(x)\right|^2\\ &\leqslant C\left|\int_{\partial B_R} \mathrm{e}^{-\mathrm{i}\xi\cdot x}\left(\partial_\nu u\right)\mathrm{d}s(x)\right|^2 + C\left|\int_{\partial B_R} \mathrm{e}^{-\mathrm{i}\xi\cdot x}\left(i\xi\cdot\nu u\right)\mathrm{d}s(x)\right|^2\\ &\leqslant Ck^8\|u\|^2_{H^{1/2}(\partial B_R)}.\end{aligned} \tag{3.21}$$

Here $C > 0$ is independent of k. Hence

$$|\widehat{f_k}(\xi_1)|^2 = \left|\frac{1}{\sqrt{2\pi}}\int_{-R}^{R} f(x_1,k)\,\mathrm{e}^{-\mathrm{i}\xi_1\cdot x_1}\mathrm{d}x_1\right|^2 \leqslant Ck^8\epsilon^2 \quad \text{for all} \quad |\xi_1| < k. \tag{3.22}$$

Denote

$$I_1(s) = \int_{|\xi_1|\leqslant s} |\widehat{f_k}(\xi_1)|^2\mathrm{d}\xi_1, s > 0.$$

Let $\xi_1 = s\hat{\xi}_1$ for $\hat{\xi}_1 \in (-1,1)$. It is easy to get

$$I_1(s) = \int_{|\xi_1|\leqslant s} |\widehat{f_k}(\xi_1)|^2 \mathrm{d}\xi_1 = \int_{-1}^{1} |\widehat{f_k}\left(s\hat{\xi}_1\right)|^2 s\mathrm{d}\hat{\xi}_1 = \frac{1}{2\pi}\int_{-1}^{1} \Big|\int_{-R}^{R} f_k(x_1)\,\mathrm{e}^{-\mathrm{i}s\hat{\xi}_1 x_1}\mathrm{d}x_1\Big|^2 s\mathrm{d}\hat{\xi}_1. \tag{3.23}$$

Since $\mathrm{e}^{-\mathrm{i}s\hat{\xi}_1 x_1}$ is an entire analytic function of $s \in \mathbb{C}$, the function I_1 can be extended analytically to the complex plane with respect to $s = s_1 + is_2 \in \mathbb{C}$, $s_1, s_2 \in \mathbb{R}$. In the following we show an upper bound estimate of I_1.

Lemma 3.1. *Let $\|f_k\|_{L^2(\mathbb{R})} \leqslant M$. We have for all $s = s_1 + is_2 \in \mathbb{C}$ that*

$$|I_1(s)| \leqslant \frac{2RM^2|s|e^{2R|s_2|}}{\pi}.$$

Proof. Recall from (3.23) that

$$I_1(s) = \frac{1}{2\pi}\int_{-1}^{1} \Big|\int_{-R}^{R} f_k(x_1)\,\mathrm{e}^{-\mathrm{i}s\hat{\xi}_1 x_1}\mathrm{d}x_1\Big|^2 s\mathrm{d}\hat{\xi}_1, \qquad s = s_1 + \mathrm{i}s_2 \in \mathbb{C}.$$

Noting the inequality $|\mathrm{e}^{-\mathrm{i}s\hat{\xi}_1 x_1}| \leqslant \mathrm{e}^{R|s_2|}$ for all $x_1 \in (-R,R)$ and $\hat{\xi}_1 \in (0,1)$, we obtain

$$\begin{aligned}
|I_1(s)| &\leqslant \frac{1}{2\pi}\int_{-1}^{1}\left(\int_{-R}^{R}|f_k(x_1)\,\mathrm{e}^{-\mathrm{i}s\hat{\xi}_1 x_1}|\mathrm{d}x_1\right)^2 |s|\mathrm{d}\hat{\xi}_1 \\
&\leqslant \frac{1}{2\pi}\int_{-1}^{1} 2R\int_{-R}^{R}|f_k(x_1)|^2|\mathrm{e}^{-\mathrm{i}s\hat{\xi}_1 x_1}|^2|s|\mathrm{d}x_1\mathrm{d}\hat{\xi}_1 \\
&\leqslant \frac{2R|s|\mathrm{e}^{2R|s_2|}}{\pi}\int_{\mathbb{R}}|f_k|^2\mathrm{d}x_1,
\end{aligned}$$

which completes the proof of lemma 3.1 by using the bound of f_k. □

Let us recall the following result on the analytical continuation proved in [11].

Lemma 3.2. *Let $J(z)$ be an analytic function in $S = \{z = x + iy \in \mathbb{C} : -\frac{\pi}{4} < \arg z < \frac{\pi}{4}\}$ and continuous in $\overline{S}$ satisfying*

$$\begin{cases} |J(z)| \leqslant \epsilon, & z \in (0, L], \\ |J(z)| \leqslant V, & z \in S, \\ |J(0)| = 0. \end{cases}$$

Then there exists a function $\mu(z)$ satisfying

$$\begin{cases} \mu(z) \geqslant \frac{1}{2}, & z \in \left(L, 2^{\frac{1}{4}}L\right), \\ \mu(z) \geqslant \frac{1}{\pi}\left(\left(\frac{z}{L}\right)^4 - 1\right)^{-\frac{1}{2}}, & z \in \left(2^{\frac{1}{4}}L, +\infty\right) \end{cases}$$

such that

$$|J(z)| \leqslant V\epsilon^{\mu(z)} \quad \textit{for all} \quad z \in (L, +\infty).$$

Using lemma 3.2, we show an upper bound of $I_1(s)$ for $s \in (k, \infty)$ in terms of the measurement data ϵ and M.

Lemma 3.3. *Let* $\|f_k\|_{L^2(\mathbb{R})} \leqslant M$. *Then there exists a function* $\mu(s)$ *satisfying*

$$\begin{cases} \mu(s) \geqslant \frac{1}{2}, & s \in \left(k, 2^{\frac{1}{4}}k\right), \\ \mu(s) \geqslant \frac{1}{\pi}\left(\left(\frac{s}{k}\right)^4 - 1\right)^{-\frac{1}{2}}, & s \in \left(2^{\frac{1}{4}}k, +\infty\right) \end{cases}$$

such that

$$|I_1(s)| \leqslant CM^2k^9e^{(2R+1)s}\epsilon^{2\mu(s)} \quad \text{for all } k < s < +\infty, \tag{3.24}$$

where $C > 0$ *depends on* R *and* δ.

Proof. Let the sector $S \subset \mathbb{C}$ be given in lemma 3.2. Observe that $|s_2| \leqslant s_1$ when $s \in S$. It follows from lemma 3.1 that

$$|I_1(s)\,\mathrm{e}^{-(2R+1)s}| \leqslant CM^2,$$

where $C > 0$ depends on R. Recalling the a prior estimate (3.22), we obtain

$$|I_1(s)| \leqslant Cs^9\epsilon^2 \leqslant Ck^9\epsilon^2, \quad s \in [0,k], \tag{3.25}$$

with $C > 0$ depending on R and δ. Hence

$$\left|\frac{1}{k^9}I_1(s)\,\mathrm{e}^{-(2R+1)s}\right| \leqslant C\epsilon^2 \quad \text{for all } s \in [0,k].$$

Then applying lemma 3.2 with $L = k$ to the function $J(s) := \frac{1}{k^9}I_1(s)\mathrm{e}^{-(2R+1)s}$, we conclude that there exists a function $\mu(s)$ satisfying

$$\begin{cases} \mu(s) \geqslant \frac{1}{2}, & s \in \left(k, 2^{\frac{1}{4}}k\right), \\ \mu(s) \geqslant \frac{1}{\pi}\left(\left(\frac{s}{k}\right)^4 - 1\right)^{-\frac{1}{2}}, & s \in \left(2^{\frac{1}{4}}k, \infty\right) \end{cases}$$

such that

$$\left|\frac{1}{k^9}I_1(s)\,\mathrm{e}^{-(2R+1)s}\right| \leqslant CM^2\epsilon^{2\mu(s)},$$

where $k < s < +\infty$ and C depends on R and δ. Thus we complete the proof. □

Proof of theorem 3.1. If $\epsilon \geqslant \mathrm{e}^{-1}$, then the bound (3.19) is straightforward. If $\epsilon < \mathrm{e}^{-1}$, we discuss (3.19) in two cases as follows.

Case (i): $2^{\frac{1}{4}}((2R+3)\pi)^{\frac{1}{3}}k^{\frac{1}{3}} < |\ln\epsilon|^{\frac{1}{4}}$. Choose $s_0 = \frac{1}{((2R+3)\pi)^{\frac{1}{3}}}k^{\frac{2}{3}}|\ln\epsilon|^{\frac{1}{4}}$. It is easy to get $s_0 > 2^{\frac{1}{4}}k$, which implies

$$-\mu(s_0) \leqslant -\frac{1}{\pi}\left(\left(\frac{s_0}{k}\right)^4 - 1\right)^{-\frac{1}{2}} \leqslant -\frac{1}{\pi}\left(\frac{k}{s_0}\right)^2.$$

A direct application of estimate (3.24) shows that

$$\begin{aligned} |I_1(s_0)| &\leqslant CM^2k^9\epsilon^{2\mu(s_0)}\mathrm{e}^{(2R+3)s_0} \\ &\leqslant CM^2k^9\mathrm{e}^{(2R+3)s_0 - 2\mu(s_0)|\ln\epsilon|} \\ &\leqslant CM^2k^9\mathrm{e}^{(2R+3)s_0 - \frac{2|\ln\epsilon|}{\pi}\left(\frac{k}{s_0}\right)^2} \\ &= CM^2k^9\mathrm{e}^{-2\left(\frac{(2R+3)^2}{\pi}\right)^{\frac{1}{3}}k^{\frac{2}{3}}|\ln\epsilon|^{\frac{1}{2}}\left(1-\frac{1}{2}|\ln\epsilon|^{-\frac{1}{4}}\right)}. \end{aligned}$$

Noting that $1-\frac{1}{2}|\ln\epsilon|^{-\frac{1}{4}}>\frac{1}{2}$ and $(\frac{(2R+3)^2}{\pi})^{\frac{1}{3}}>1$, we have

$$|I_1(s_0)|\leqslant CM^2k^9\mathrm{e}^{-k^{\frac{2}{3}}|\ln\epsilon|^{\frac{1}{2}}}.$$

Using the inequality $\mathrm{e}^{-t}\leqslant\frac{16!}{t^{16}}$ for $t>0$, we get

$$|I_1(s_0)|\leqslant C\frac{M^2k^9}{\left(k^{\frac{2}{3}}|\ln\epsilon|^{\frac{1}{2}}\right)^{16}}\leqslant C\frac{M^2}{k^{\frac{5}{3}}|\ln\epsilon|^8}.$$

It is clear that $k^{\frac{5}{3}}|\ln\epsilon|^8\geqslant k^{\frac{4}{3}}|\ln\epsilon|^{\frac{1}{2}}$ when $k\geqslant 1$ and $|\ln\epsilon|\geqslant 1$. Obviously, the following inequalities holds

$$\begin{aligned}\int_{|\xi_1|>s_0}|\widehat{f_k}(\xi_1)|^2\mathrm{d}\xi_1&=s_0^{-2}\int_{|\xi_1|>s_0}\xi_1^2|\widehat{f_k}(\xi_1)|^2\mathrm{d}\xi_1\\&\leqslant s_0^{-2}\int_{\mathbb{R}}|\widehat{\nabla f_k}(\xi_1)|^2\mathrm{d}\xi_1=s_0^{-2}\int_{\mathbb{R}}|\nabla f_k(\xi_1)|^2\mathrm{d}\xi_1\leqslant\frac{M^2}{s_0^2}\end{aligned}$$

by the Parseval's identity. Hence

$$\begin{aligned}\|f_k\|^2_{L^2(\mathbb{R})}=\|\widehat{f_k}\|^2_{L^2(\mathbb{R})}&=I_1(s_0)+\int_{|\xi_1|>s_0}|\widehat{f_k}(\xi_1)|^2\mathrm{d}\xi_1\\&\leqslant I_1(s_0)+\frac{M^2}{s_0^2}\\&\leqslant C\left(\frac{M^2}{k^{\frac{5}{3}}|\ln\epsilon|^8}+\frac{M^2}{k^{\frac{4}{3}}|\ln\epsilon|^{\frac{1}{2}}}\right)\\&\leqslant C\frac{M^2}{k^{\frac{4}{3}}|\ln\epsilon|^{\frac{1}{2}}}.\end{aligned}\tag{3.26}$$

Case (ii):$|\ln\epsilon|^{\frac{1}{4}}\leqslant 2^{\frac{1}{4}}((2R+3)\pi)^{\frac{1}{3}}k^{\frac{1}{3}}$. In this case we choose $s_0=k$. Then we find $s_0\geqslant 2^{-\frac{1}{4}}((2R+3)\pi)^{-\frac{1}{3}}k^{\frac{2}{3}}|\ln\epsilon|^{\frac{1}{4}}$. Using the estimate (3.25) gives $|I_1(s_0)|\leqslant Ck^9\epsilon^2$. Hence

$$\begin{aligned}\|f_k\|^2_{L^2(\mathbb{R})}=\|\widehat{f_k}\|^2_{L^2(\mathbb{R})}&=I_1(s_0)+\int_{|\xi_1|>s_0}|\widehat{f_k}(\xi_1)|^2\mathrm{d}\xi_1\\&\leqslant I_1(s_0)+\frac{M^2}{s_0^2}\\&\leqslant C\left(k^9\epsilon^2+\frac{M^2}{k^{\frac{4}{3}}|\ln\epsilon|^{\frac{1}{2}}}\right)\\&\leqslant C\left(k^9\epsilon^2+\frac{M^2}{k^{\frac{4}{3}}|\ln\epsilon|^{\frac{1}{2}}}\right).\end{aligned}\tag{3.27}$$

Combining (3.26) and (3.27), we finally get

$$\|f_k\|^2_{L^2(\mathbb{R})}\leqslant C\left(k^9\epsilon^2+\frac{M^2}{k^{\frac{4}{3}}|\ln\epsilon|^{\frac{1}{2}}}\right).$$

The proof of theorem 3.1 is complete. □

4. Numerical examples

In this section, we present some numerical results in $\mathbb{R}^2$. Our objective is to demonstrate the feasibility and effectiveness of the two reconstruction methods proposed in section 2. The synthetic observation data are generated by solving the direct problem (1.4) and (1.5). The radiated multi-frequency data are measured on the boundary of a circular region centered at $x_0 \in \mathbb{R}^2$ with radius R. By coordinate translation we write $u(r,\theta;k) = u(x;k)$ in polar coordinates, where $r = |x - x_0| \geqslant 0$ and $\theta \in (0, 2\pi)$ denotes the angle between $x - x_0$ with the positive real axis. Below we set $B_R := B_R(x_0)$. Then the boundary data can be obtained through the integral expression

$$u(R,\theta;k) = \int_{\mathrm{B}_R} \Phi(x-y;k) f(y_1,k) g(y_2) \mathrm{d}y, \quad \theta \in (0,2\pi], k \in [k_{\min}, k_{\max}]. \tag{4.28}$$

The Neumann data is obtained through the Dirichlet-to-Neumann map,

$$\partial_\nu u(R,\theta;k) = \sum_{n=-\infty}^{+\infty} k \frac{H_n^{(1)\prime}(kR)}{H_n^{(1)}(kR)} u_n(R,k) \mathrm{e}^{\mathrm{i}n\theta}, \quad \theta \in (0,2\pi], k \in [k_{\min}, k_{\max}], \tag{4.29}$$

where $H_n^{(1)}(\cdot)$ denotes the first kind Hankel function of order n, $H_n^{(1)\prime}(\cdot)$ is the first derivative of $H_n^{(1)}(\cdot)$ and $u_n(R,k)$ is calculated using the Fourier series representation

$$u_n(R,k) = \frac{1}{2\pi} \int_0^{2\pi} u(R,\theta;k)\, \mathrm{e}^{-\mathrm{i}n\theta} \mathrm{d}\theta, \quad k \in [k_{\min}, k_{\max}].$$

The noise polluted data $u^\delta(R,\theta;k)$ are generated by

$$u^\delta(R,\theta;k) = u(R,\theta;k) + \delta\zeta |u(R,\theta;k)|, \quad \theta \in (0,2\pi], k \in [k_{\min}, k_{\max}], \tag{4.30}$$

where ζ is a uniformly distributed random number within the range $[-1,1]$ and δ represents the noise level. The Neumann data with noise can be computed similarly by

$$\partial_\nu u^\delta(R,\theta;k) = \sum_{n=-\infty}^{+\infty} k \frac{H_n^{(1)\prime}(kR)}{H_n^{(1)}(kR)} u_n^\delta(R,k) \mathrm{e}^{\mathrm{i}n\theta}, \quad \theta \in (0,2\pi], k \in [k_{\min}, k_{\max}],$$

where $u_n^\delta(R,k)$ denote the Fourier coefficients of $u^\delta(R,\theta;k)$.

Now we provide details of our numerical implementation and carry out a series of experiments in two dimensions. In our work, we set the lower bound of the wave-number as $k_{\min} = K/J$ and the upper bound as $k_{\max} = K$ for some $K > 0$ and $J \in \mathbb{N}$. The discrete radiated field data are collected as follows:

$$\{u(R,\theta_m;k_j) : \theta_m = 2\pi m/M, k_j = jK/J, m = 1,2,\ldots,M, j = 1,2,\ldots,J\}. \tag{4.31}$$

Note that the boundary data are measured on the circle $\partial \mathrm{B}_R(x_0)$ centered at $x_0 = (\pi/2, 0)$ with the radius of $R = \pi/2$. Additionally, we calculate the Neumann data by using the formula defined in (4.29) as follows:

$$\{\partial_\nu u(R,\theta_m;k_j) : \theta_m = 2\pi m/M, k_j = jK/J, m = 1,2,\ldots,M, j = 1,2,\ldots,J\}. \tag{4.32}$$

Unless otherwise specified, we always set $M = 100$ in our experiments. In figure 1, we show the support of the source $f(x_1,k)g(x_2)$ for $k \in [k_{\min}, k_{\max}]$ along with the depiction of the measurement boundary $\partial \mathrm{B}_R(x_0)$. For the sake of simplicity, we assume that $g(x_2) = 1$ if $x_2 \in [-\pi/4, \pi/4]$ and $g = 0$ if else.

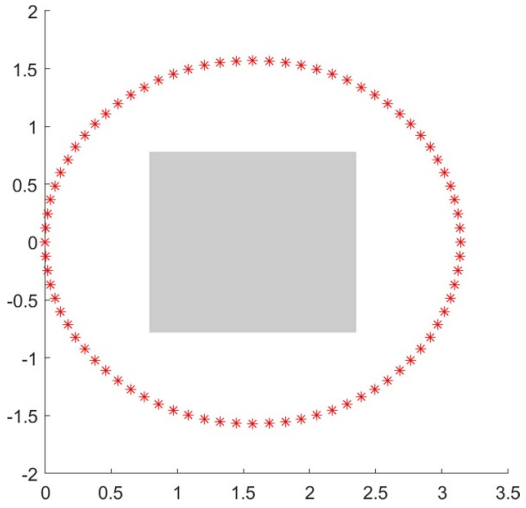

Figure 1. The gray rectangle represents the source support, where $\operatorname{supp} f(\cdot,k) = [\pi/4, 3\pi/4]$ and $\operatorname{supp} g(\cdot) = [-\pi/4, \pi/4]$. The red arsterisks show the measurement positions lying on the circle centered at $x_0 = (\pi/2, 0)$ with the radius $R = \pi/2$.

4.1. Numerical implementation by Dirichlet-Laplacian method

In this subsection, by using the expansion defined in (2.10), we reconstruct the exact source $f(\cdot,k) \in L^2(0,\pi)$ for some fixed $k \in [K/J, K]$. To achieve this, one can opt for the eigenfunctions of the Dirichlet Laplacian, as they form a complete and orthonormal basis in the space $L^2(0,\pi)$. Consider the one-dimensional eigenvalue problem

$$\begin{cases} -v''(x_1) = \lambda^2 v(x_1), & x_1 \in [0,\pi], \\ v(x_1) = 0, & x_1 = 0, \pi. \end{cases} \tag{4.33}$$

We obtain the Dirichlet eigenvalues $\{n^2 : |n| \in \mathbb{N}^+\}$ and the eigenfunctions $\{\sin(nx_1) : |n| \in \mathbb{N}^+\}$. To get the expansion (2.10), we choose a suitably large value N. By substituting the eigenvalues and eigenfunctions into (2.12), i.e. with $\varphi_n = \sin(nx_1)\mathrm{e}^{\sqrt{n^2-k^2}x_2}$ for $|n| \leqslant N$ in (2.12), one can deduce that

$$\begin{aligned} &\int_{\mathrm{B}_R} f(x_1,k)\, g(x_2) \sin(nx_1)\, \mathrm{e}^{\sqrt{n^2-k^2}x_2} \mathrm{d}x \\ &= \int_{\partial \mathrm{B}_R} \left\{ \partial_\nu u(x,k) \sin(nx_1)\, \mathrm{e}^{\sqrt{n^2-k^2}x_2} - u(x,k)\, \partial_\nu \left(\sin(nx_1)\, \mathrm{e}^{\sqrt{n^2-k^2}x_2} \right) \right\} \mathrm{d}s(x). \end{aligned}$$

Note that $B_R = B_R(x_0)$ with $x_0 = (\pi/2, 0)$ in our experiments. It implies that

$$\int_0^\pi f(x_1,k_j) \sin(nx_1)\, \mathrm{d}x_1 = \frac{M_{n,j}}{G_{n,j}} \tag{4.34}$$

for $n = \pm 1, \pm 2, \cdots, \pm N$ and $j = 1, 2, \cdots, J$, where

$$M_{n,j} := \int_{\partial \mathrm{B}_R} \left\{ \partial_\nu u(x,k_j) \sin(nx_1)\, \mathrm{e}^{\sqrt{n^2-k_j^2}x_2} - u(x,k_j)\, \partial_\nu \left(\sin(nx_1)\, \mathrm{e}^{\sqrt{n^2-k_j^2}x_2} \right) \right\} \mathrm{d}s(x),$$

$$G_{n,j} := \int_{-\frac{\pi}{4}}^{\frac{\pi}{4}} g(x_2)\, \mathrm{e}^{\sqrt{n^2-k_j^2}x_2} \mathrm{d}x_2.$$

Algorithm 1. Dirichlet-Laplacian method in $\mathbb{R}^2$.

Require: $g(x_2)$, $k_{\min}$, $k_{\max}$, H, M, R, J, δ, N
Ensure: f_N
1: Collect the measurement data u and compute the Neumann data $\partial_\nu u$;
2: Calculate the Dirichlet eigenfunctions $\{v_n\}_{|n|\in\mathbb{N}^+}$ of the negative Laplacian operator on $\widetilde{B}_R$;
3: Compute the expansion coefficients:

$$\begin{aligned} f_{n,j} &= \frac{1}{|\widetilde{B}_R|}\int_{\widetilde{B}_R} f(x_1,k_j)v_n(x_1)\,\mathrm{d}x_1. \\ &= \frac{1}{|\widetilde{B}_R|}\frac{\int_{\partial B_R}[\partial_\nu u v_n - u\partial_\nu v_n]\,\mathrm{d}s(x)}{\int_H g(x_2)\mathrm{e}^{\sqrt{\lambda_n^2-k_j^2}x_2}\mathrm{d}x_2}, \end{aligned}$$

where (λ_n, v_n) are the spectral data.
4: Reconstruction formula:

$$f_N(x_1,k_j) = \sum_{|n|\leqslant N} f_{n,j}v_n(x_1), \quad j = 1,2,\cdots,J.$$

We approximate $M_{n,j}$ through the discrete measurement data in polar coordinates as defined in (4.31) and (4.32). The reconstructed source $f(x_1,k_j)$ can be approximated by $f_N(x_1,k_j)$ for all $x_1 \in [0,\pi]$,

$$f_N(x_1,k_j) = 2\sum_{n=1}^{N} f_{n,j}\sin(nx_1). \tag{4.35}$$

Here we have used the relation $f_{n,j} = -f_{-n,j}$ for $n \in \mathbb{N}$. By (4.34) and (4.35), one can compute the coefficients $f_{n,j}$ from the measurement data as follows:

$$f_{n,j} = \frac{1}{\pi}\int_0^\pi f(x_1,k_j)\sin(nx_1)\,\mathrm{d}x_1 = \frac{1}{\pi}\frac{M_{n,j}}{G_{n,j}}, \tag{4.36}$$

provided $G_{n,j} \neq 0$ for all $n = 1,2,\cdots,N$ and $j = 1,2,\cdots,J$. Similarly, the reconstruction formula using noise data is given by

$$f_N^\delta(x_1,k_j) = 2\sum_{n=1}^{N} f_{n,j}^\delta \sin(nx_1), \quad f_{n,j}^\delta := \frac{1}{\pi}\frac{M_{n,j}^\delta}{G_{n,j}}, \tag{4.37}$$

for all $n = 1,2,\cdots,N$ and $j = 1,2,\cdots,J$, with

$$M_{n,j}^\delta := \int_{\partial \mathrm{B}_R}\left\{\partial_\nu u^\delta(x,k_j)\sin(nx_1)\mathrm{e}^{\sqrt{n^2-k_j^2}x_2} - u^\delta(x,k_j)\,\partial_\nu\left(\sin(nx_1)\mathrm{e}^{\sqrt{n^2-k_j^2}x_2}\right)\right\}\mathrm{d}s(x).$$

The algorithm is summarized as algorithm 1.

Using formulas (4.35) and (4.36), we demonstrate the reconstructions of the following source functions when $k = 0.5$:

$$f^{(1)}(x_1,k) = \begin{cases} \mathrm{e}^{-20k(x_1-\pi/2)^2}, & x_1 \in \left[\frac{\pi}{4},\frac{3\pi}{4}\right], \\ 0, & \text{otherwise}, \end{cases} \tag{4.38}$$

$$f^{(2)}(x_1,k) = \begin{cases} \cos(4kx_1), & x_1 \in \left[\frac{\pi}{4},\frac{3\pi}{4}\right], \\ 0, & \text{otherwise}, \end{cases} \tag{4.39}$$

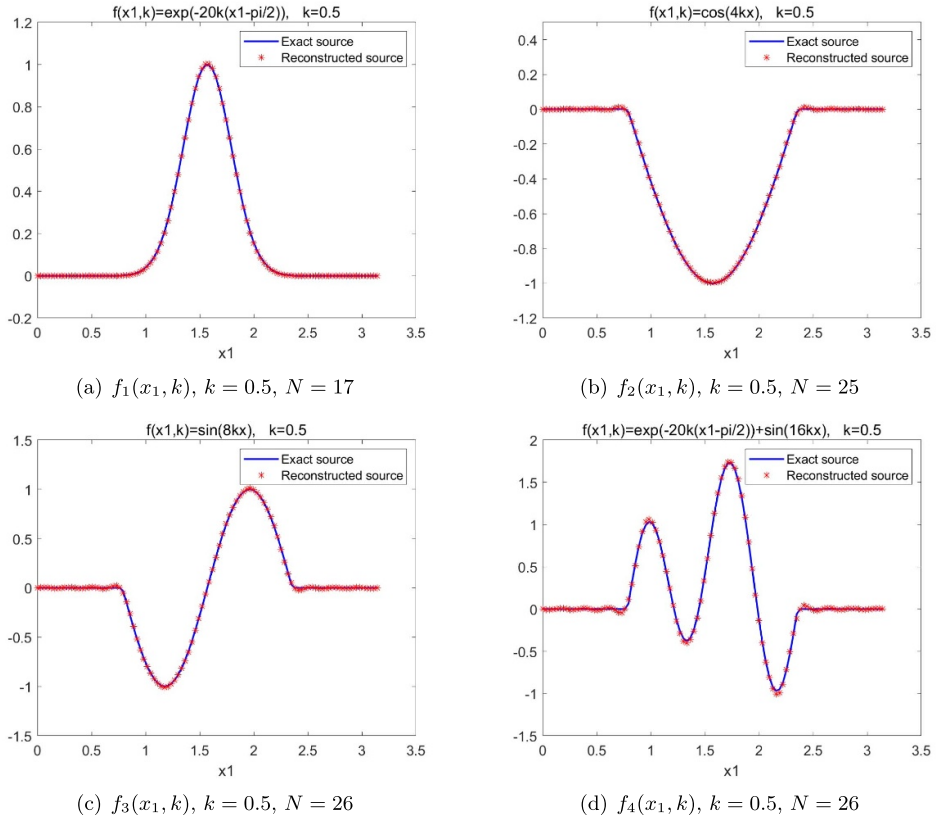

(a) $f_1(x_1,k)$, $k=0.5$, $N=17$ (b) $f_2(x_1,k)$, $k=0.5$, $N=25$

(c) $f_3(x_1,k)$, $k=0.5$, $N=26$ (d) $f_4(x_1,k)$, $k=0.5$, $N=26$

Figure 2. The reconstructed sources $f_N^{(j)}(x_1,k)$ by the Dirichlet-Laplacian method with a fixed $k=0.5$. The exact source functions are $f^{(j)}(x_1,k)$ $(j=1,2,3,4)$ in (a)–(d), with the truncated parameter N chosen as $N=17$, 25, 26, 26, respectively.

$$f^{(3)}(x_1,k)=\begin{cases}\sin(8kx_1), & x_1\in\left[\frac{\pi}{4},\frac{3\pi}{4}\right],\\ 0, & \text{otherwise},\end{cases}$$

$$f^{(4)}(x_1,k)=\begin{cases}\mathrm{e}^{-20k(x_1-\pi/2)^2}+\sin(8kx_1), & x_1\in\left[\frac{\pi}{4},\frac{3\pi}{4}\right],\\ 0, & \text{otherwise}.\end{cases}$$

It is obvious that the source can be well reconstructed by choosing an appropriate parameter N in figure 2. We use the source function $f^{(1)}(x_1,0.5)$ to generate the noise-free radiation field data on $\partial\mathrm{B}_R$. The reconstructed source of $f^{(1)}(x_1,0.5)$ is displayed in figure 2(a) with $N=17$. In figure 2(b), the source function $f^{(2)}(x_1,0.5)$ can be well reconstructed with $N=25$. Choosing the source function $f^{(3)}(x_1,0.5)$ and $N=26$, we obtain the reconstruction results in figure 2(c). If the source function is $f^{(4)}(x_1,0.5)$ and $N=26$, we get the reconstructed result in figure 2(d).

However, the above method fails in the case $G_{n,j}=0$, because the denominator on the right side of (4.36) vanishes. For example, in reconstructing the source function $f^{(1)}(x_1,1)$ with $N=10$, or the source function

$$f^{(5)}(x_1,3)=\begin{cases}\cos(2x_1), & x_1\in\left[\frac{\pi}{4},\frac{3\pi}{4}\right],\\ 0, & \text{otherwise},\end{cases}$$

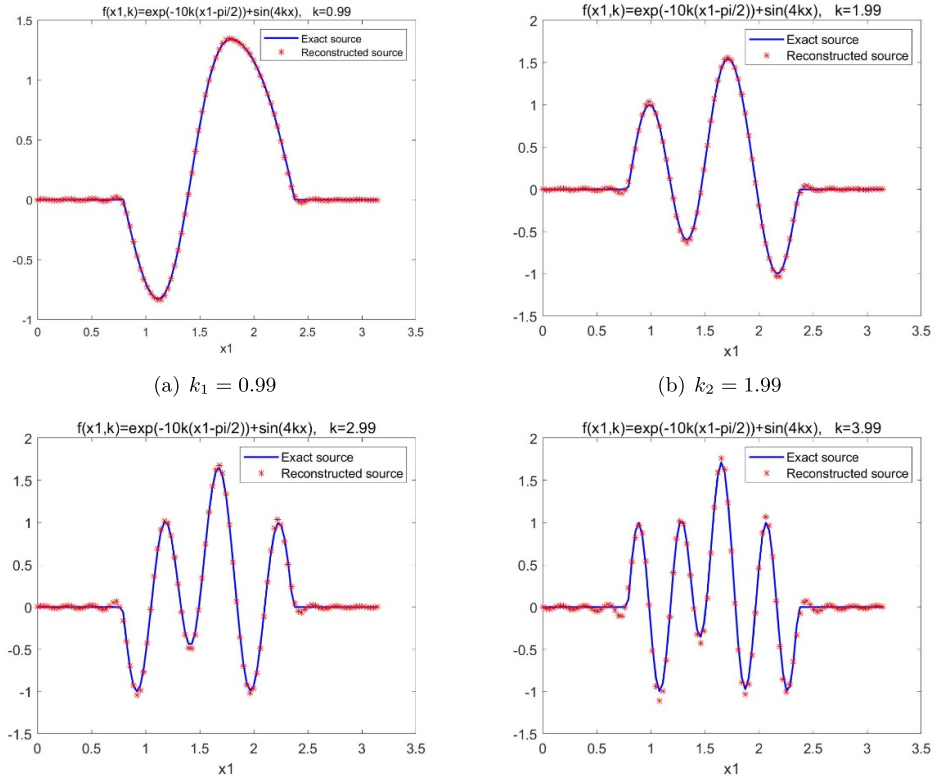

(a) $k_1 = 0.99$ (b) $k_2 = 1.99$

(c) $k_3 = 2.99$ (d) $k_4 = 3.99$

Figure 3. The recovery of the source function $x_1 \mapsto \mathrm{e}^{-10k_j(x_1-\pi/2)^2} + \sin(4k_j x_1)$ for $x_1 \in [\pi/4, 3\pi/4]$ by the Dirichlet-Laplacian method with $N = 26$. Here we use four different wave-numbers $k_1 = 0.99$, $k_2 = 1.99$, $k_3 = 2.99$ and $k_4 = 3.99$.

with $N = 10$, one cannot obtain a correct reconstruction. We refer to the end of this section for possible solutions to overcome this difficulty.

Next, we choose different wave-numbers $0 < k \notin \mathbb{N}^+$ to test the effectiveness of the Dirichlet-Laplacian method. Figure 3 illustrates that the source function $\mathrm{e}^{-10k(x_1-\pi/2)^2} + \sin(4kx_1)$ supported in $[\pi/4, 3\pi/4]$ can be well reconstructed for various wave-numbers $0 < k \notin \mathbb{N}^+$. When $k_1 = 0.99$ and $N = 26$ (as shown in figure 3(a)), it is evident that the reconstructed source closely matches the exact source. In other cases, such as $k_2 = 1.99$ and $N = 26$; $k_3 = 2.99$ and $N = 26$; $k_4 = 3.99$ and $N = 26$, we also achieve satisfactory reconstructions.

Finally, we examine the sensitivity of the Dirichlet-Laplacain method to random noise. The measurement data (4.28) is polluted by random noise using the formula (4.30). Figure 4 displays the reconstructions f_N^δ of the source function $f = \sin(8kx_1)$ supported in $[\pi/4, 3\pi/4]$ with noise levels $\delta = 0.5\%$, $\delta = 2\%$, $\delta = 10\%$ and $\delta = 30\%$. It can be concluded that the error decreases as the noise level decreases, where the error is defined as

$$\text{error} = \frac{\|f - f_N^\delta\|_2}{\|f\|_2}. \tag{4.40}$$

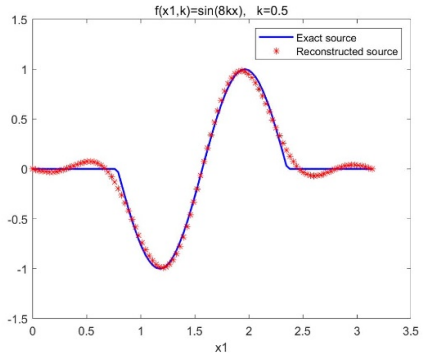

(a) $\delta = 0.5\%$, $N = 6$, error $= 0.1015$

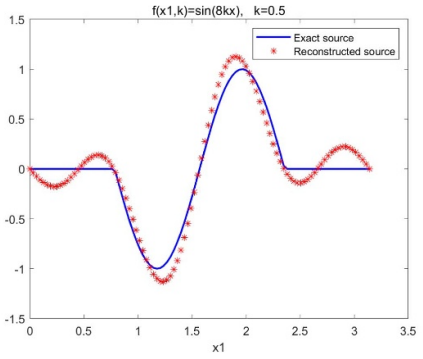

(b) $\delta = 2\%$, $N = 6$, error $= 0.2226$

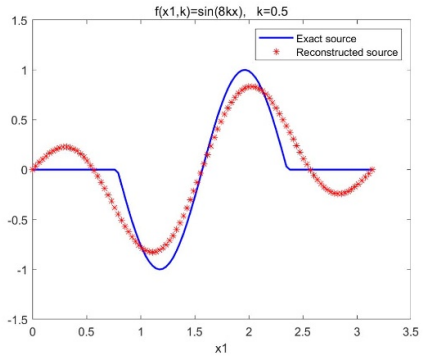

(c) $\delta = 10\%$, $N = 4$, error $= 0.3739$

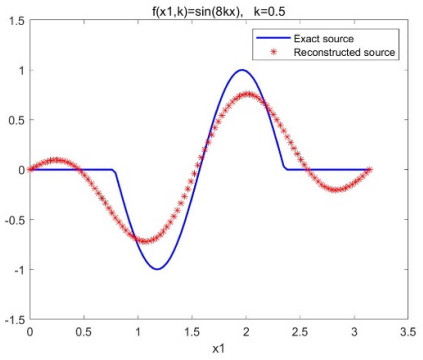

(d) $\delta = 30\%$, $N = 4$, error $= 0.4383$

Figure 4. The reconstructed source by the Dirichlet-Laplacian method with different noise levels δ.

4.2. Numerical implementation by Fourier-transform method

The purpose of this subsection is to reconstruct the exact source $f(\cdot,k) \in L^2(0,\pi)$ for some $k>0$ by using the Fourier expansion. A computational formula for each Fourier coefficient is derived. We still consider the source function shown in figure 1. According to (2.7), the Fourier basis functions over $L^2[0,\pi]$ are given by

$$\mathrm{e}^{\mathrm{i}\xi_1 x_1}, \quad \xi_1 = 2n,\ n \in \mathbb{Z},$$

since $\xi_1 = \frac{2\pi}{2R} n = 2n$ by our choice $R = \pi/2$. Next, we establish computational formulas for the Fourier coefficients of $f(x_1,k) \in L^2[0,\pi]$ under the Fourier basis functions $\{\mathrm{e}^{\mathrm{i}(2n)x_1} : x_1 \in [0,\pi], n \in \mathbb{Z}\}$. By (2.8), we obtain

$$\int_{\mathrm{B}_R} f(x_1,k)\, g(x_2)\, \mathrm{e}^{-\mathrm{i}(\xi_1 x_1 + \xi_2 x_2)} \mathrm{d}x = \int_{\partial \mathrm{B}_R} \{\partial_\nu u(x,k) + \mathrm{i}\xi \cdot \nu u(x,k)\}\, \mathrm{e}^{-\mathrm{i}(\xi_1 x_1 + \xi_2 x_2)} \mathrm{d}s(x)$$

where $\xi_1^2 + \xi_2^2 = k^2$, $k>0$. Set $k = k_j$ for some $j = 1,2,\cdots,J$. A simple calculation yields that

$$\int_0^\pi f(x_1,k_j)\, \mathrm{e}^{-\mathrm{i}(2n)x_1} \mathrm{d}x_1 = \frac{\tilde{M}_{n,j}}{\tilde{G}_{n,j}} \tag{4.41}$$

Algorithm 2. Fourier-transform method.

Requuire: $g(x_2)$, k, H, M, R, J, δ, N
Ensure: $\widetilde{f}_N(x_1,k)$
1: Collect the measurement data u and compute $\partial_\nu u$;
2: Describe the Fourier basis functions in $\widetilde{B}_R$:

$$\mathrm{e}^{\mathrm{i}\xi_1 x_1}, \qquad \xi_1 = \frac{2n\pi}{|\widetilde{B}_R|}, \quad n \in \mathbb{N};$$

3: Calculate the expansion coefficients:

$$\begin{aligned}\tilde{f}_n &= \frac{1}{|\widetilde{B}_R|}\int_{|\widetilde{B}_R|} f(x_1,k)\mathrm{e}^{-\mathrm{i}\xi_1 x_1}\mathrm{d}x_1 \\ &= \frac{1}{|\widetilde{B}_R|}\frac{\int_{\partial B_R}\left[\partial_\nu u\,\mathrm{e}^{-\mathrm{i}\xi_1 x_1} - u\partial_\nu \mathrm{e}^{-\mathrm{i}\xi_1 x_1}\right]\mathrm{d}s\,(x)}{\int_H g(x_2)\mathrm{e}^{-\mathrm{i}\xi_2 x_2}\mathrm{d}x_2}\end{aligned}$$

for all $|n| \leqslant N$, where $\xi_2^2 = k^2 - \xi_1^2$.
4: Reconstruction formula:

$$\tilde{f}_N(x_1,k) = \sum_{|n|\leqslant N}\tilde{f}_n \mathrm{e}^{\mathrm{i}\xi_1 x_1}, \quad \xi_1 = \frac{2n\pi}{|\widetilde{B}_R|}.$$

for $n \in \mathbb{Z}$ and $j = 1,2,\cdots,J$, where $\tilde{M}_{n,j}$ and $\tilde{G}_{n,j}$ are defined as

$$\tilde{M}_{n,j} := \int_{\partial \mathrm{B}_R}\left\{\partial_\nu u(x,k_j) + i\left(2n, \sqrt{k_j^2 - 4n^2}\right)\cdot \nu u(x,k_j)\right\}\mathrm{e}^{-\mathrm{i}\left(2nx_1 + \sqrt{k_j^2-4n^2}x_2\right)}\mathrm{d}s\,(x),$$

$$\tilde{G}_{n,j} := \int_{-\frac{\pi}{4}}^{\frac{\pi}{4}} g\,(x_2)\,\mathrm{e}^{-\mathrm{i}\sqrt{k_j^2-4n^2}x_2}\mathrm{d}x_2.$$

The reconstructed source $\tilde{f}_N(x_1,k_j)$ with $x_1 \in [0,\pi]$, $k_j \in [K/J,K]$ can be written as

$$\tilde{f}_N(x_1,k_j) = \sum_{|n|\leqslant N}\tilde{f}_{n,j}\mathrm{e}^{\mathrm{i}(2n)x_1}. \tag{4.42}$$

From (4.41), the coefficients are approximated by

$$\tilde{f}_{n,j} \approx \frac{1}{\pi}\int_0^\pi f(x_1,k_j)\,\mathrm{e}^{-\mathrm{i}(2n)x_1}\mathrm{d}x_1 = \frac{1}{\pi}\frac{\tilde{M}_{n,j}}{\tilde{G}_{n,j}}, \quad n \in \mathbb{Z}, j = 1,2,\cdots,J, \tag{4.43}$$

where the denominator is again assumed to be non-vanishing. Similarly, the reconstruction formula from noise data is given by

$$\tilde{f}_N^\delta(x_1,k_j) = \sum_{|n|\leqslant N}\tilde{f}_{n,j}\mathrm{e}^{\mathrm{i}(2n)x_1}, \quad x_1 \in [0,\pi], k_j \in [0,K],$$

$$\tilde{f}_{n,j}^\delta \approx \frac{1}{\pi}\frac{\tilde{M}_{n,j}^\delta}{\tilde{G}_{n,j}}, \quad n \in \mathbb{Z}, j = 1,2,\cdots,J,$$

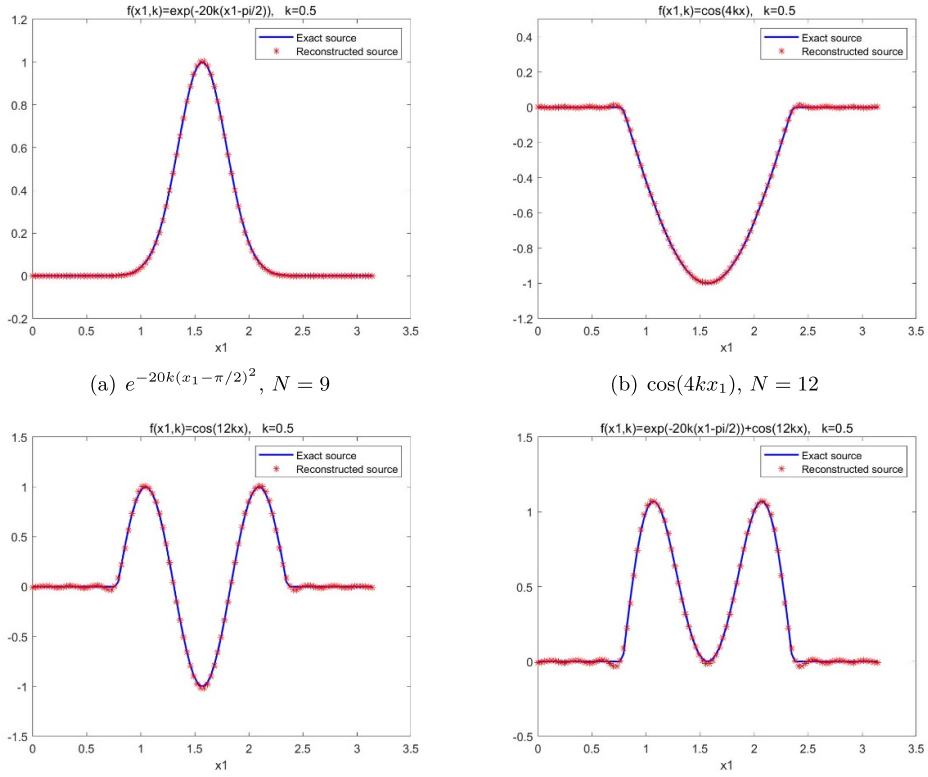

(a) $e^{-20k(x_1-\pi/2)^2}$, $N=9$ (b) $\cos(4kx_1)$, $N=12$

(c) $\cos(12kx_1)$, $N=12$ (d) $e^{-20k(x_1-\pi/2)^2}+\cos(12kx_1)$, $N=12$

Figure 5. The reconstructed source by the Fourier-transform method with $k=0.5$. Four different sources are reconstructed with $N=9$, 12, 12, 12, respectively.

where

$$\tilde{M}^{\delta}_{n,j}:=\int_{\partial \mathrm{B}_R}\left\{\partial_\nu u^{\delta}(x,k_j)+\mathrm{i}\left(2n,\sqrt{k_j^2-4n^2}\right)\cdot\nu u^{\delta}(x,k_j)\right\}\mathrm{e}^{-\mathrm{i}\left(2nx_1+\sqrt{k_j^2-4n^2}x_2\right)}\mathrm{d}s(x).$$

We call the above reconstruction method the Fourier-transform method, which is described as the algorithm 2.

Using formulas (4.42) and (4.43), we present the reconstructions when $k=0.5$. Choosing the source function $f^{(1)}(x_1,k)$ in (4.38) with $N=9$, the reconstructed results are shown in figure 5(a). In figure 5(b), the source function $f^{(2)}(x_1,k)$ with $N=12$ is well reconstructed. For source function $\cos(12kx_1)$ supported in $[\pi/4,3\pi/4]$ with $N=12$, the experimental results shown in figure 5(c) demonstrate that the reconstructed sources closely resemble the exact one; In figure 2(d), the source function $\mathrm{e}^{-20k(x_1-\pi/2)^2}+\cos(12kx_1)$ supported in $[\pi/4,3\pi/4]$ with $N=12$ is well reconstructed.

It is important to note that for $k=2n$, $n\in\mathbb{N}^+$, the source function cannot be reconstructed due to the vanishing of $\tilde{G}_{n,j}$. However, by approximating such wave-numbers $k=2n$ with $k=2n\pm\varepsilon$, $0<\varepsilon\ll 1$, $n\in\mathbb{N}^+$, figure 6(b) displays a successful reconstruction of $\cos(kx_1)$ supported in $[\pi/4,3\pi/4]$ with $k=2$. Following this, we apply the Fourier-transform method to the source $\mathrm{e}^{-5k(x_1-\pi/2)^2}$ by using different wave-numbers. The recovery results are presented in figure 7. The recreated image in figure 7(a) closely resembles the exact source function with

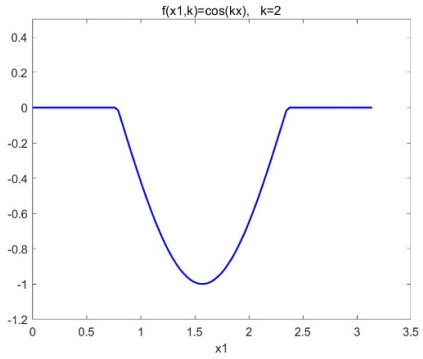

(a) $\cos(kx_1)$, $k = 2$, $N = 12$

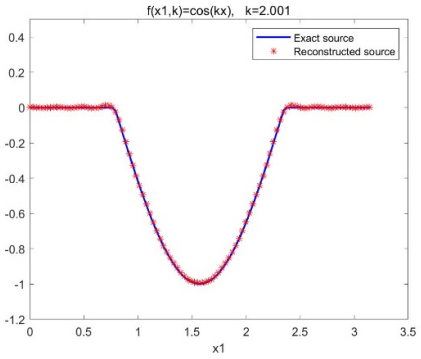

(b) $\cos(kx_1)$, $k = 2.001$, $N = 12$

Figure 6. The reconstructed source by the Fourier-transform method with $N = 12$. The left shows the exact source function with $k = 2$, while the right shows the reconstruction result with $k = 2.001$.

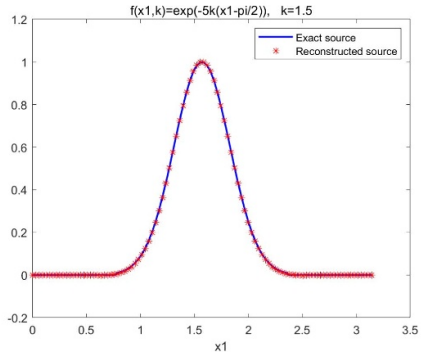

(a) $k = 1.5$, $N = 8$

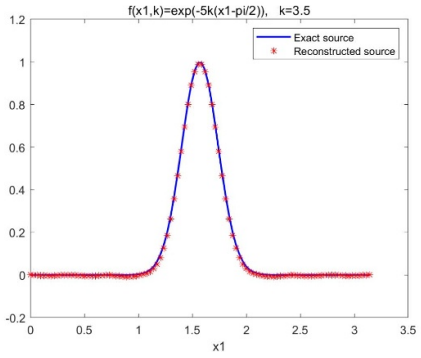

(b) $k = 3.5$, $N = 8$

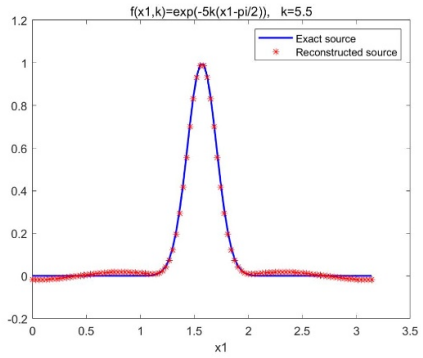

(c) $k = 5.5$, $N = 13$

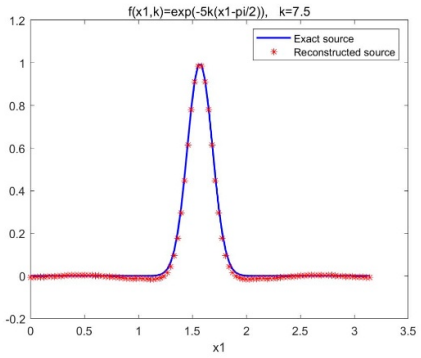

(d) $k = 7.5$, $N = 13$

Figure 7. The reconstructed source using the Fourier-transform method for the exact source $e^{-5k(x_1-\pi/2)^2}$. Each figure corresponds to a different value of k.

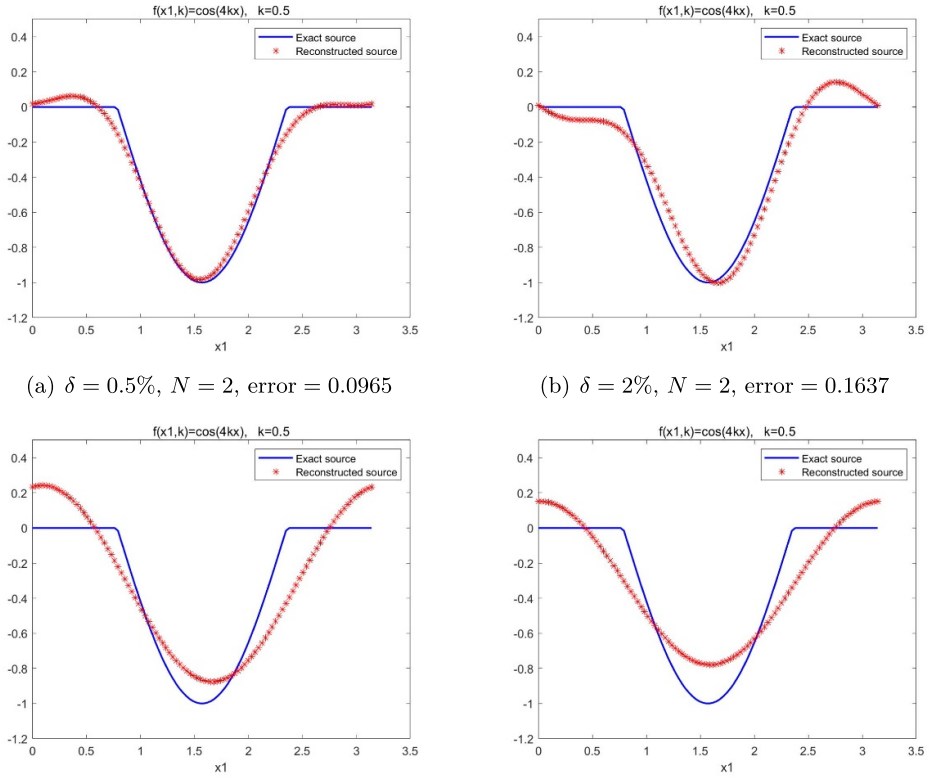

(a) $\delta = 0.5\%$, $N = 2$, error $= 0.0965$ (b) $\delta = 2\%$, $N = 2$, error $= 0.1637$

(c) $\delta = 10\%$, $N = 1$, error $= 0.3516$ (d) $\delta = 20\%$, $N = 1$, error $= 0.4106$

Figure 8. The reconstructed sources using the Fourier-transform method with different noise levels δ.

$k = 1.5$ and $N = 8$. In figure 7(b), employing $k = 3.5$ and $N = 8$ for the source reconstruction yields favorable results. Subsequently, figures 7(c) and (d) display the reconstructed sources with $k = 5.5$, $N = 13$ and $k = 7.5$, $N = 13$, respectively. It is evident from these figures that as the wave-number k increases, the recovery effect becomes slightly less accurate.

At the end, we investigate the impact of noise on the Fourier-transform method. The measurement data (4.28) is polluted by random noise using the formula (4.30). Different noise levels, $\delta = 0.5\%$, $\delta = 2\%$, $\delta = 10\%$ and $\delta = 20\%$, are introduced. Figure 8 illustrates the recreated results, indicating that the reconstruction error decreases as the noise level decreases, where the error is again defined by (4.40).

5. Conclusion

In this paper, we have established uniqueness, increasing stability and algorithms for an inverse wave-number-dependent source problem. In d-dimensions, the unknown source function depends on $\tilde{x} = (x_1, \cdots, x_{d-1})$ and k but independent of x_d. The Fourier-transform method, grounded in the Fourier basis, ensures both uniqueness and stability. The Dirichlet-Laplacian method is based on the Dirichlet eigenfunctions, but its stability remains to be further examined. Two efficient non-iterative numerical algorithms have been developed. A possible

continuation of this work is to investigate the stability under incomplete data and explore scenarios involving other kinds of wave-number-dependent sources.

Data availability statement

All data that support the findings of this study are included within the article (and any supplementary files).

Acknowledgment

The work of G Hu is partially supported by the National Natural Science Foundation of China (No. 12071236) and the Fundamental Research Funds for Central Universities in China (No. 63233071). The work of S Si is supported by Shandong Provincial Natural Science Foundation (No. ZR2022QA111).

ORCID iDs

Mengjie Zhao https://orcid.org/0000-0003-4946-9646
Suliang Si https://orcid.org/0000-0002-7831-4187
Guanghui Hu https://orcid.org/0000-0002-8485-9896

References

[1] Acosta S, Chow S, Taylor J and Villamizar V 2012 On the multi-frequency inverse source problem in heterogeneous media *Inverse Problems* **28** 075013
[2] Alzaalig A, Hu G, Liu X and Sun J 2020 Fast acoustic source imaging using multi-frequency sparse data *Inverse Problems* **36** 025009
[3] Arridge S 1999 Optical tomography in medical imaging *Inverse Problems* **15** 41–93
[4] Bao G, Li P and Lin J 2015 Inverse scattering problems with multi-frequencies *Inverse Problems* **31** 093001
[5] Bao G, Lin J and Triki F 2010 A multi-frequency inverse source problem *J. Differ. Equ.* **249** 3443–65
[6] Bao G, Lu S, Rundell W and Xu B 2015 A recursive algorithm for multi-frequency acoustic inverse source problems *SIAM J. Numer. Anal.* **53** 1608–28
[7] Bao G, Liu Y and Triki F 2021 Recovering point sources for the inhomogeneous Helmholtz equation *Inverse Problems* **37** 095005
[8] Bellassoued M and Yamamoto M 2017 *Carleman Estimates and Applications to Inverse Problems for Hyperbolic Systems* (Springer)
[9] Bellassoued M and Ben Aicha I 2017 Stable determination outside a cloaking region of two time-dependent coefficients in an hyperbolic equation from Dirichlet to Neumann map *J. Math. Anal. Appl.* **229** 46–76
[10] Bleistein N and Cohen J 1977 Nonuniqueness in the inverse source problem in acoustics and electromagnetics *J. Math. Phys.* **18** 194–201
[11] Cheng J, Isakov V and Lu S 2017 Increasing stability in the inverse source problem with many frequencies *J. Differ. Equ.* **260** 4786–804
[12] Choudhury A P and Heck H 2018 Increasing stability for the inverse problem for the Schrödinger equation *Math. Methods Appl. Sci.* **41** 606–14
[13] Colton D and Kress R 2013 *Inverse Acoustic and Electromagnetic Scattering Theorey* 3rd edn (Springer)
[14] Chandler-Wilde S N and Monk P 2008 Wave-number-explicit bounds in time-harmonic scattering *SIAM J. Math. Anal.* **39** 1428–55
[15] Eller M and Valdivia N 2009 Acoustic source identification using multiple frequency information *Inverse Problems* **25** 115005

[16] Entekhabi M 2018 Increasing stability in the two dimensional inverse source scattering problem with attenuation and many frequencies *Inverse Problems* **34** 115001
[17] Entekhabi M and Isakov V 2020 Increasing stability in acoustic and elastic inverse source problems *SIAM J. Math. Anal.* **52** 5232–56
[18] Fokas A, Kurylev Y and Marinakis V 2015 The unique determination of neuronal currents in the brain via magnetoencephalography *Inverse Problems* **20** 1067–82
[19] Guo H and Hu G 2024 Inverse wave-number-dependent source problems for the Helmholtz equation *SIAM Numer. Anal.* **62** 1372–93
[20] Guo H, Hu G and Zhao M 2023 Direct sampling method to inverse wave-number-dependent source problems: determination of the support of a stationary source *Inverse Problems* **39** 105008
[21] Harrison B 2000 An inverse problem in underwater acoustic source localization: robust matched-field processing *Inverse Problems* **16** 1641
[22] Hu G and Kian Y 2020 Uniqueness and stability for the recovery of a time-dependent source and initial conditions in elastodynamics *Inverse Problems Imaging* **14** 463–87
[23] Hu G, Kian Y and Zhao Y 2020 Uniqueness to some inverse source problems for the wave equation in unbounded domains *Acta Math. Appl. Sin. Engl.* **36** 134–50
[24] Isakov V and Lu S 2018 Inverse source problems without (pseudo) convexity assumptions *Inverse Problems Imaging* **12** 955–70
[25] Isakov V 2007 Increasing stability in the continuation for the Helmholtz equation with variable coefficient *Comtemp. Math.* **426** 255–69
[26] Isakov V 2017 *Inverse Problems for Partial Differential Equations* (Springer)
[27] Isakov V, Nagayasu S, Uhlmann G and Wang J-N 2014 Increasing stability of the inverse boundary value problem for the Schrödinger equation *Contemp. Math.* **615** 131–41
[28] Li P and Yuan G 2017 Increasing stability for the inverse source scattering problem with multi-frequencies *Inverse Problems Imaging* **11** 745–59
[29] Li P, Zhai J and Zhao Y 2020 Stability for the acoustic inverse source problem in inhomogeneous media *SIAM J. Appl. Math.* **80** 2547–59
[30] McLean W 2000 *Strongly Elliptic Systems and Boundary Integral Equations* (Cambridge University Press) pp 288–9
[31] Stefanov P and Uhlmann G 2011 Themoacoustic tomography arising in brain imaging *Inverse Problems* **27** 075011
[32] Zhang D and Guo Y 2020 Fourier method for solving the multi-frequency inverse source problem for the Helmholtz equation *Inverse Problems* **36** 463–87